



## 저작자표시-비영리-변경금지 2.0 대한민국

이용자는 아래의 조건을 따르는 경우에 한하여 자유롭게

- 이 저작물을 복제, 배포, 전송, 전시, 공연 및 방송할 수 있습니다.

다음과 같은 조건을 따라야 합니다:



저작자표시. 귀하는 원저작자를 표시하여야 합니다.



비영리. 귀하는 이 저작물을 영리 목적으로 이용할 수 없습니다.



변경금지. 귀하는 이 저작물을 개작, 변형 또는 가공할 수 없습니다.

- 귀하는, 이 저작물의 재이용이나 배포의 경우, 이 저작물에 적용된 이용허락조건을 명확하게 나타내어야 합니다.
- 저작권자로부터 별도의 허가를 받으면 이러한 조건들은 적용되지 않습니다.

저작권법에 따른 이용자의 권리는 위의 내용에 의하여 영향을 받지 않습니다.

이것은 [이용허락규약\(Legal Code\)](#)을 이해하기 쉽게 요약한 것입니다.

[Disclaimer](#)

의학박사 학위논문

**Synergistic Anti-Skin Aging Effect of  
Adipose-derived Stem Cell and Fat Graft  
in Aged Mice**

노화된 생쥐에서 지방줄기세포와  
지방이식의 항피부노화 상승효과

2018 년 8 월

서울대학교 대학원

의학과 성형외과학 전공

김 기 갑

## **ABSTRACT**

# **Synergistic Anti-Skin Aging Effect of Adipose-derived Stem Cell and Fat Graft in Aged Mice**

**Kikap Kim**

**College of Medicine**

**Department of Plastic and Reconstructive Surgery**

**The Graduate School**

**Seoul National University**

**Background:** We investigated the beneficial effects of adipose-derived stem cells (ADSCs) and fat graft on skin wrinkles in a nude mouse model of chronological aging.

**Methods:** With 50 weeks of chronological aging, 44 female BALB/c-nude mice were classified into 4 groups, i.e., a negative control group and groups injected subcutaneously with ADSCs (1

$\times 10^5$  cells in 0.5 ml) on the back, injected with fat tissue (0.5 ml), or injected with both fat tissue (0.5 ml) and ADSCs ( $1 \times 10^5$  cells in 0.5ml). The degree of wrinkling was evaluated by a replica analysis and skin biopsies were performed after 4 weeks. The dermal thickness and density of collagen were determined. The levels of type 1 collagen and MMP were determined by western blot and type 1 procollagen mRNA levels were evaluated by RT-PCR. Tropoelastin, fibrillin-1, and CD31 were evaluated by immunohistochemistry.

**Results:** Based on the total wrinkle area, there was significant wrinkle reduction in the fat group and the ADSC with fat group. Collagen expression and type I procollagen mRNA levels were significantly higher in the ADSC with fat group than in the ADSC group and in the fat group. In addition, the ADSC with fat group exhibited significantly higher CD31 expression levels than those in the ADSC group and in the fat group.

**Conclusions:** ADSCs and fat could both play important roles in wrinkle reduction and have synergic effects on collagen synthesis and neovascularization.

---

**Keywords:** Stem cells, Mesenchymal Stem Cells, Fat graft, Aging of Skin

**Student Number:** 2011-30537

## List of Figures

Figure 1. Total wrinkle area of nude mouse according to age -----	13
Figure 2. Gross pictures -----	14
Figure 3. Skin replica analysis -----	15
Figure 4. Skin replica analysis -----	16
Figure 5. Dermal thickness -----	17
Figure 6. Dermal thickness -----	18
Figure 7. The density of collagen -----	19
Figure 8. The density of collagen -----	20
Figure 9. Type I procollagen mRNA -----	21
Figure 10. Tropoelastin -----	22
Figure 11. Fibrillin-1 -----	23
Figure 12. Expression of CD31-----	24
Figure 13. Expression of CD31-----	25
Figure 14. The numbers of CD31-positive vessels -----	26

# CONTENTS

<b>Abstract</b> ·····	i
<b>List of figures</b> ·····	iii
<b>I . Introduction</b> ·····	1
<b>II . Materials and Methods</b> ·····	3
<b>III. Results</b> ·····	9
<b>IV. Discussion</b> ·····	27
<b>V . Conclusion</b> ·····	32
<b>References</b> ·····	33
<b>Abstract in Korean</b> ·····	40

## INTRODUCTION

Various studies have focused on improving wrinkles.<sup>1</sup> Animal models have been developed to confirm wrinkle-improving effects, and these have been used to establish the effects of particular cell types, e.g., fat, adipose-derived stem cells (ADSC), and fibroblasts.<sup>2-12</sup>

Skin aging can be divided into endogenous aging over time and extrinsic aging caused by extreme stress, ultraviolet rays, and smoking.<sup>2,3</sup> After long-term UV exposure, the epidermis and dermis are thickened and wrinkles form.<sup>2,4</sup> In these photoaged skins, the number and function of fibroblasts decrease and the structural stability of the dermis is destroyed.<sup>4,5</sup> Recently, the anti-aging effects of adult stem cells, such as ADSCs, have been proven in photoaging models and these cells are emerging as a new anti-aging solution.<sup>6-9</sup> The injection of cultured stem cells could be used to regenerate aged skin by transplanting self-derived cells that can directly induce skin substrates. In addition, adipocyte stem cells release cytokines, growth factors, and other molecules that exert paracrine effects.<sup>13-15</sup> There is significant recent interest in the properties and effects of ADSCs.<sup>6-9</sup> Subcutaneously injected ADSCs effectively increase collagen synthesis, collagen density, fibroblast density, and dermal thickness during

photoaging.<sup>16</sup> Additional studies have shown that ADSCs increase levels of procollagen type I and decrease levels of matrix metalloproteinases (MMPs), thereby increasing the dermal collagen density.<sup>8,9,16</sup> Therefore, a proposed mechanism by which ADSCs reduce wrinkles involves collagen generation, decreased MMP expression, and fibroblast activation.<sup>8,9,16</sup>

Several clinical studies have shown that it is more effective to use ADSCs together with fat graft than to use fat graft alone.<sup>17,18</sup> Although most reports are clinical case series, they suggest that the injection of cultured ADSCs and fat graft could play an important role in anti-aging therapy.<sup>19</sup> However, the mechanism underlying wrinkle improvement has not been evaluated. In addition, comparative analyses of the effects of fat injection only and the injection of fat and ADSCs together on wrinkles are lacking. We evaluated wrinkles using a chronological aging model, rather than a photo-aged model, which has been widely used in the past. Using this model, we verified the effects of the injection of fat tissues and ADSCs and the injection of fat tissues alone in a comparative framework.



## **MATERIALS AND METHODS**

### **Isolation and culture of ADSCs**

Abdominal adipose tissue samples were obtained from discarded tissues from a 48-year-old woman who underwent transverse rectus abdominis myocutaneous flap surgery for breast reconstruction. Samples were collected after obtaining informed consent and the study protocols were approved by the Seoul National University Hospital Institutional Review Board (No. H-1108-098-374).<sup>7,16</sup> The fat was suction aspirated from the discarded tissue and washed twice using phosphate-buffered saline (PBS). The samples were processed with 0.1% collagenase type I (Worthington Biochemicals, Lakewood, NJ, USA) under agitation at 37°C and centrifuged for 10 minutes at  $800 \times g$ . The centrifuged pellet was then washed and re-suspended in PBS.<sup>7,16</sup> After repeat centrifugation, the supernatant was removed and the cell band that was buoyant over Histopaque was collected.<sup>6</sup> Cells were cultured overnight at 37°C and 5% CO<sub>2</sub> in control medium (10% fetal bovine serum, 100 IU penicillin, 100 mg/ml streptomycin, 5 µg/ml heparin, and 2 ng/ml acidic fibroblast factor).<sup>8</sup> The adherent cell population containing ADSCs was maintained over 3 days and then expanded and cultured.<sup>8</sup>

## **Animal experiments**

Fifty-six 6-week-old female BALB/c nude mice were provided by ORIENT Inc. (Seongnam, Korea). The hypothesis of inferiority was rejected in the lower bound of the 95% confidence interval if it exceeded  $-20\%$ . The mice were nourished on a standardized diet for 1 week prior to the experiment. A total of 52 mice were assigned to 4 groups: a negative control group, fat group, ADSC group, and fat with ADSC group.<sup>20</sup> The animals were fed until 50 weeks of age and subjected to treatments. Mice in the negative control group received no injection. In the fat group, 0.5 cc of fat was injected in the dorsal skin wrinkles of the mice. The fat graft subset was centrifuged at 1200 rpm for 3 min as in routine fat graft, followed by oil and blood removal and injected using 18-gauge needles with 1 cc syringes. In the ADSC group, 0.5 cc of ADSCs ( $1 \times 10^5$  cells) were injected in the dorsal skin wrinkles of the mice.<sup>21</sup> A 26-gauge needles were used for the injection of cells diluted in 0.5 ml Hank's Balanced Salt Solution (HBSS). In the fat with ADSC group, 0.5 cc of fat were injected using 18-gauge needles with 1 cc syringes and ADSC ( $1 \times 10^5$  cells diluted in 0.5 ml Hank's Balanced Salt) were injected using 26-gauge needles into the dorsal skin wrinkles of the mice. The injection volume of  $1 \times 10^5$  cells was chosen based on the results of previous experiments.<sup>21</sup> All injections were made parallel to deep wrinkles in a retrograde fashion

into the subdermal and panniculus adiposus planes. Three to five injections were administered per mouse. Mice were monitored for 4 weeks after injection.<sup>21</sup> This animal study was monitored and approved by the Institutional Animal Care and Use Committee of the Seoul National University (IACUC Protocol No. 13-0228-C2A0).

## **Evaluation**

Wrinkles were evaluated by preparing impressions of the dorsal skin surfaces with a silicon-based impression material (Courage + Khazaka Electronic GmbH, Koln, Germany). The impressions were cut into 1-cm-diameter discs and rotated to achieve oblique illumination. A high-resolution Visioline<sup>®</sup> VL 650 camera (Courage + Khazaka Electronic GmbH) was used to detect vertical shadows within the prepared discs. The length and depth of the shadows were measured for quantitative comparisons. The total wrinkle area, mean depth, total length, and maximal depth of the dorsal skin were measured prior to and 4 weeks after injection.

At 4 weeks following injection, a 1 cm × 1 cm section of injected dorsal skin was obtained and fixed with a 10% formalin solution for histopathology.<sup>8</sup> The skin samples were embedded in wax and sectioned at 5 µm. The sections were stained with hematoxylin & eosin (H&E) and Masson's trichrome stain. Dermal thickness was

evaluated on H&E-stained sections with the averages of five measurements were obtained. Collagen density was evaluated on Masson's trichrome-stained sections using image analysis software (Leica Qwin V3 and Leica Microsystems CMS GmbH, Wetzlar, Germany) and averages of five measurements were obtained. Elastic fiber density was evaluated on Gomori's aldehyde fuchsin-stained sections using image analysis software (Leica Qwin V3 and Leica Microsystems CMS GmbH) and averages of five measurements were obtained.

To evaluate changes in gene expression, mRNA levels of various genes were measured in the skin samples. Ribonucleic acid (RNA) was isolated from specimens (50 mg) using TRIzol reagent (500 µl) and a homogenizer, resuspended in RNase-free water, and quantified using a UV spectrophotometer.<sup>16</sup> Single-stranded cDNA was prepared from 1 µg of total RNA in a 20-µl reaction volume using a TOPscript RT DryMIX (Enzynomics, Daejeon, Korea).<sup>16</sup> Real-time PCR was performed using an ABI 7500 machine with SYBR Premix Ex Taq<sup>TM</sup> (TaKaRa, Shiga, Japan). PCR conditions were as follows: 30 s at 95°C, followed by 34 cycles of 5 s at 95°C and 34 s at 60°C.<sup>22</sup> The average threshold cycle for each gene was determined from triplicate reactions.<sup>22</sup> The gene expression levels were normalized to those of beta-actin. The genes included in the analysis were procollagen, *MMP-1*, *MMP-2*, *MMP-3*, *MMP-9*, and *MMP-13*.<sup>23-25</sup>

Protein levels in the samples were also evaluated. Tissues lysates were centrifuged for 10 min at  $14000 \times g$ , and a western blot analysis was performed using the supernatants.<sup>8,16</sup> A Bradford assay was used to measure protein concentrations.<sup>8</sup> The samples were loaded onto a 10% sodium dodecyl sulfate polyacrylamide gel.<sup>8</sup> The protein samples were transferred electrophoretically to polyvinylidene difluoride membranes.<sup>8</sup> The membranes were blocked with 5% skim milk in Tris-buffered saline and Tween-20 and were incubated with the following antibodies: anti-mouse collagen type 1 (Millipore, Billerica, MA, USA), anti-MMP 1 (Novus Biologicals Inc., Littleton, CO, USA), anti-MMP 2, anti-MMP 3, anti-MMP 9, anti-MMP 13, and anti-Beta Actin (Abcam, Cambridge, MA, USA) to allow for protein visualization by enhanced chemiluminescence (Thermo Scientific, Rockford, IL, USA).<sup>16</sup> All real-time PCR and western blot analyses were performed three times per mouse gene or protein.

The samples were sectioned as previously described and sections were placed on slides and prepared using the Discovery XT Automated Immunohistochemistry Stainer (Ventana Medical Systems, Inc., Tucson, AZ, USA).<sup>26</sup> The Ventana Chromo Map Kit (Ventana Medical Systems) was used for detection.<sup>26</sup> The tissue sections were deparaffinized, and CC1 standard (pH 8.4 buffer containing Tris/Borate/EDTA) was

used to retrieve the antigen.<sup>26</sup> Inhibitor D (3% H<sub>2</sub>O<sub>2</sub>, endogenous peroxidase) was plugged in for 4 min at 37°C.<sup>27</sup> The slides were incubated with anti-Tropoelastin (Abcam) for 32 min at 37°C, and a secondary antibody, OmniMap anti-Mouse HRP, for 20 min at 37°C.<sup>24</sup> Other slides were incubated with anti-fibrillin-1 (Abcam) for 32 min at 37°C, and a an OmniMap anti-Mouse HRP secondary antibody for 20 min at 37°C.<sup>27</sup> The slides were incubated in DAB + H<sub>2</sub>O<sub>2</sub> substrate for 8 min at 37°C followed by hematoxylin and bluing reagent for counterstaining at 37°C.<sup>27</sup> A Tris buffer solution (pH 7.6) was used for washing.<sup>27</sup> The immunohistochemically stained slides were evaluated by densitometric analysis using image analysis software (Leica Qwin V3 and Leica Microsystems CMS GmbH) and averages of five measurements were obtained. Capillary density was also measured by immunohistochemical staining for CD31. The numbers of vessels were counted and densities were analyzed using the same image analysis software.

### **Statistical analysis**

Results were analyzed using nonparametric Mann–Whitney tests. SPSS Version 21.0 (SPSS, Inc., Chicago, IL, USA) was used for statistical analyses and a *p*-value of <0.05 was considered statistically significant

## **RESULTS**

### **Characterization of ADSCs**

ADSCs were cultured from fat tissue without any problems. We identified ADSCs by comparison with their typical morphology and we confirmed the molecular phenotype of cells using a fluorescence-activated cell sorting (FACS) scanner.<sup>6-9</sup> The ADSCs expressed CD13, CD73, and CD 105, but did not express CD14, CD19, CD34, CD45, and HLA-DR.

### **Chronological aging model of nude mice**

We confirmed that the total wrinkle area due to natural aging stabilized when BALB/c nude mice were older than 42–46 weeks, although a statistically significant increase was observed after 22 weeks (Figure 1). Therefore, the injections were performed at 50 weeks of age. Of the 56 total mice, 44 survived until week 50 and were assigned to groups as follows: control group (11 mice), ADSC group (11 mice), fat group (10 mice), and ADSC with fat group (12 mice).

### **Skin replica and image analysis**

Four weeks following injection, we obtained images and performed a skin replica analysis (Figures 2, 3). At 4 weeks after the cell injection, the total wrinkle area decreased in the 3 experimental groups. The total area of wrinkles was significantly lower in the fat group and ADSC with fat group than in other groups ( $p = 0.04$  and  $p = 0.01$ , respectively, Figure 4). There was no statistically significant difference in wrinkle area between the control group and the ADSC group ( $p = 0.14$ ). The mean depth of wrinkle patterns was similar in all groups.

### **Histological findings**

The average thickness of the dermis was  $145.3 \pm 12.3 \mu\text{m}$  in the ADSC group and was  $139.3 \pm 14.4 \mu\text{m}$  in the fat group. The average thickness in the combined group was  $154.5 \pm 12.4 \mu\text{m}$  (Figure 5). The dermal thickness, as determined by hematoxylin & eosin staining, was significantly greater in both the ADSC group and ADSC with fat than in the other groups ( $p = 0.04$  and  $p = 0.03$ , respectively). However, thickness did not differ significantly between the control group and the fat group ( $p = 0.19$ , Figure 6).

The density of collagen exhibited similar patterns in all groups to the dermal thickness patterns. The average densities of collagen according to an image-based analysis of Masson's trichrome staining were  $52.3 \pm 8.2\%$  in the ADSC group,  $39.5 \pm 8.6\%$  in the



fat group, and  $60.0 \pm 12.4\%$  in the ADSC with fat group (Figure 7). The densities of collagen were significantly elevated in both ADSC group and ADSC with fat group (ADSC group,  $p < 0.01$ ; ADSC with fat group,  $p < 0.01$ ). However, collagen density did not differ significantly between the fat group and the ADSC with fat group ( $p = 0.21$ , Figure 8).

### **Real-time PCR and western blot analysis**

Real-time PCR revealed that the levels of type I procollagen increased in all 3 experimental groups compared with the control group. The ratio for the ADSC group relative to the control group was  $3.2 \pm 0.5$  ( $p < 0.01$ ) and for the fat group relative to the control group was  $1.4 \pm 0.3$  ( $p = 0.04$ ). Type I procollagen mRNA levels in the ADSC with fat group were statistically significantly higher than those in the ADSC group and fat group ( $p = 0.01$ ,  $p < 0.01$ , respectively, Figure 9). The collagen type I expression pattern revealed by western blotting was consistent with the real-time PCR results. After ADSC or fat injection, the expression level increased significantly in both groups. The increase in the ADSC with fat group was significantly greater than the increases in the ADSC group and the fat group.

### **Immunohistochemical analysis**

The amount of tropoelastin decreased after ADSC injection. Moreover, the amount of tropoelastin was significantly lower after ADSC with fat injection. However, there was no statistically significant difference between the control group and the fat group (Figure 10). Fibrillin-1 increased significantly after ADSC injection and ADSC with fat injection. However, there was no statistically significant difference between the control group and fat group (Figure 11). CD31 expression increased significantly in all three groups. CD31 expression in the ADSC with fat group differed significantly from those in the ADSC group and the fat group (Figure 12, 13). The numbers of CD31-positive vessels in the ADSC with fat groups ( $31.8 \pm 6.4$ ) were significantly higher than those in the fat group ( $15.3 \pm 7.4$ ) ( $p = 0.02$ , Figure 14).

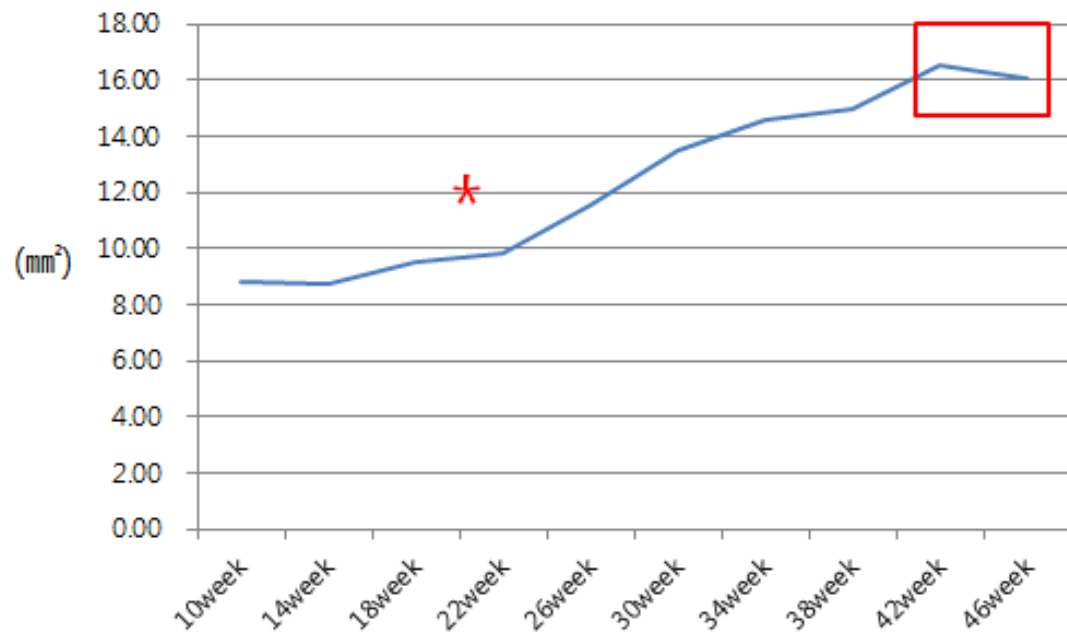


Figure 1. Total wrinkle area in nude mice according to age. We confirmed that the total wrinkle area due to natural aging stabilized when BALB/c nude mice were older than 42–46 weeks, although a statistically significant increase was observed after 22 weeks. Therefore, the injections were performed at 50 weeks of age.

## Gross pictures

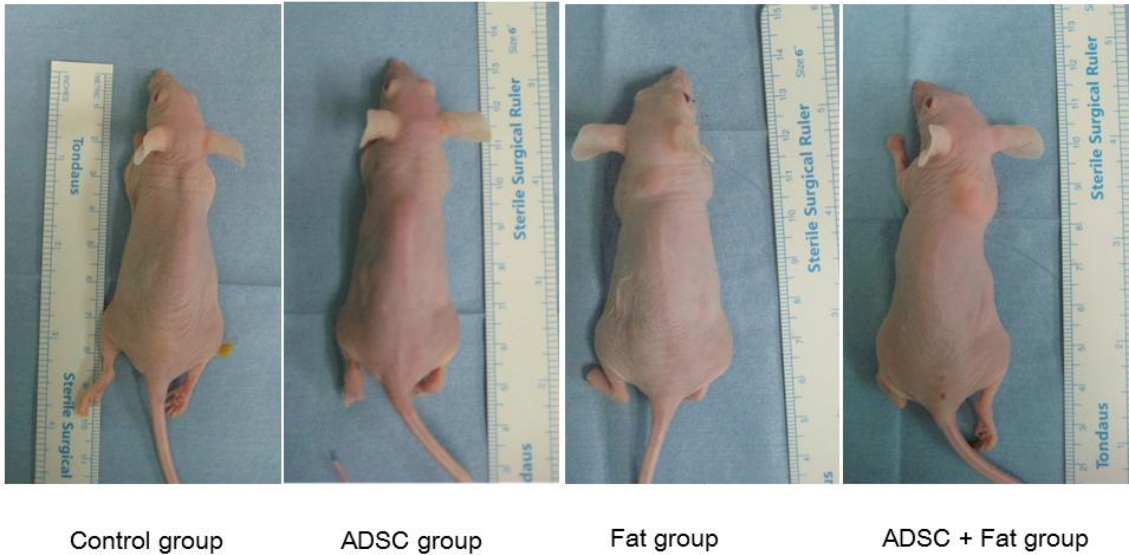


Figure 2. Gross pictures. Four weeks following injection, we obtained images.

# Replica

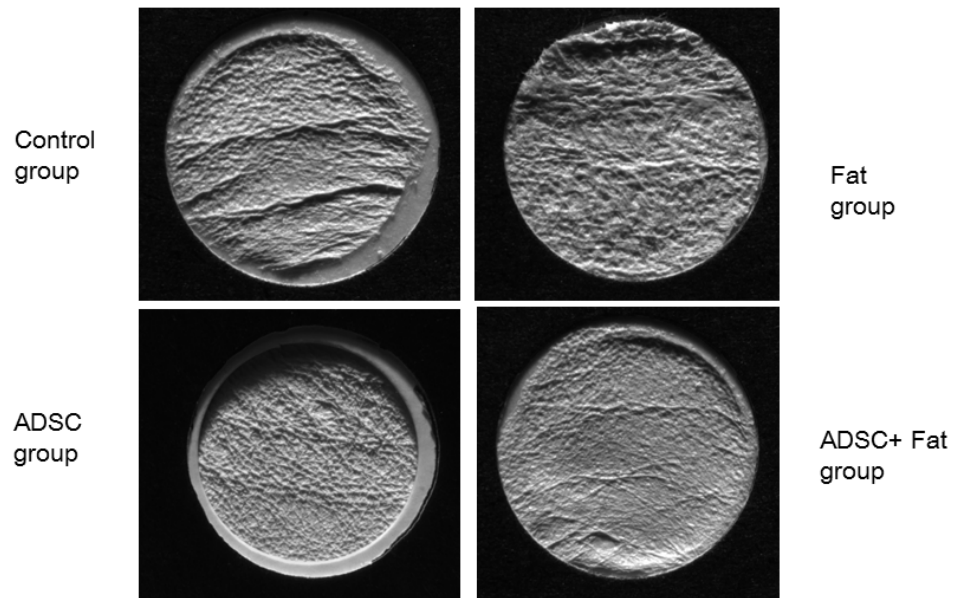


Figure 3. Skin replica analysis. Four weeks following injection, we performed a skin replica analysis.

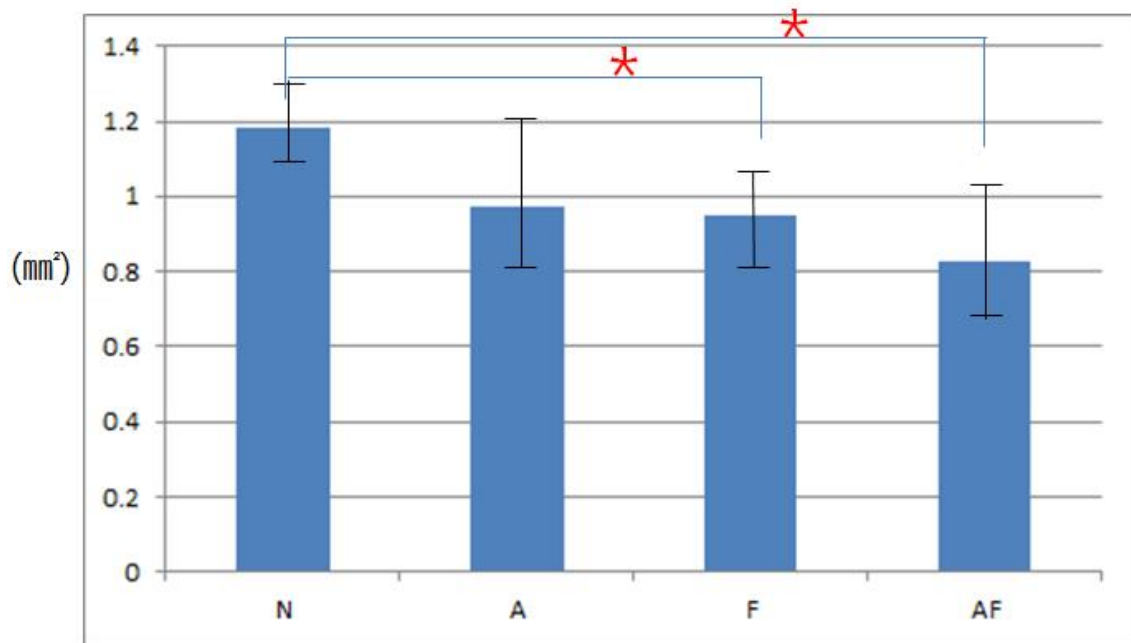


Figure 4. Skin replica analysis. At 4 weeks after the cell injection, the total wrinkle area decreased in the 3 experimental groups. The total area of wrinkles was significantly lower in the fat group and ADSC with fat group than in other groups ( $p = 0.04$  and  $p = 0.01$ , respectively). There was no statistically significant difference in wrinkle area between the control group and the ADSC group ( $p = 0.14$ ). The mean depth of wrinkle patterns was similar in all groups.

## Dermal thickness

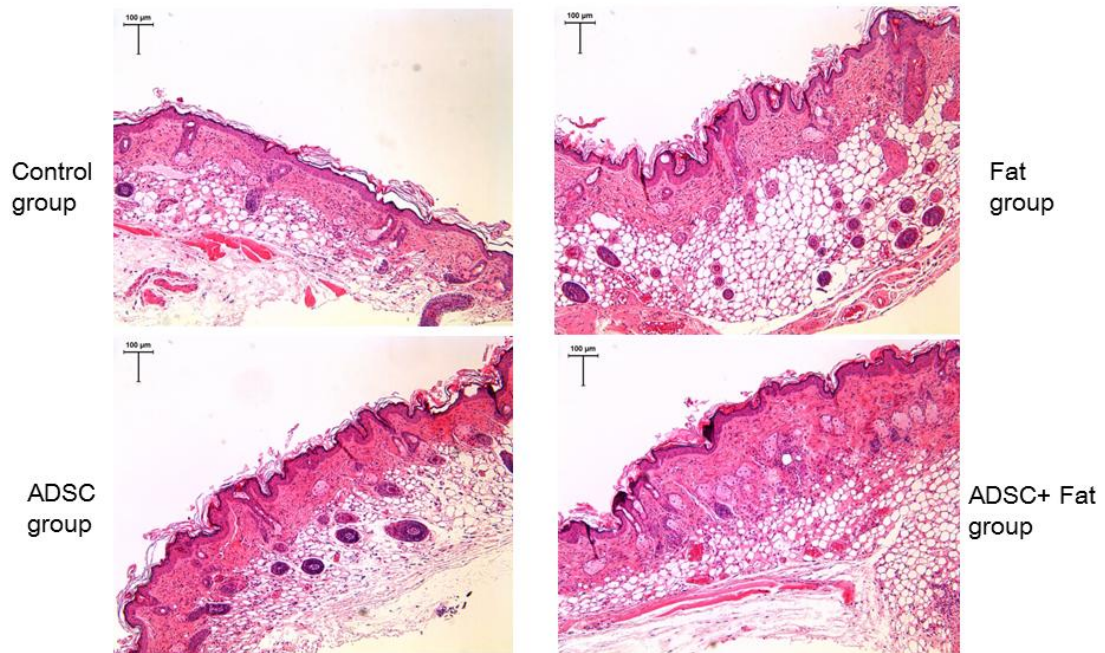


Figure 5. Dermal thickness. The average thickness of the dermis was  $145.3 \pm 12.3 \mu\text{m}$  in the ADSC group and was  $139.3 \pm 14.4 \mu\text{m}$  in the fat group. The average thickness in the combined group was  $154.5 \pm 12.4 \mu\text{m}$ .

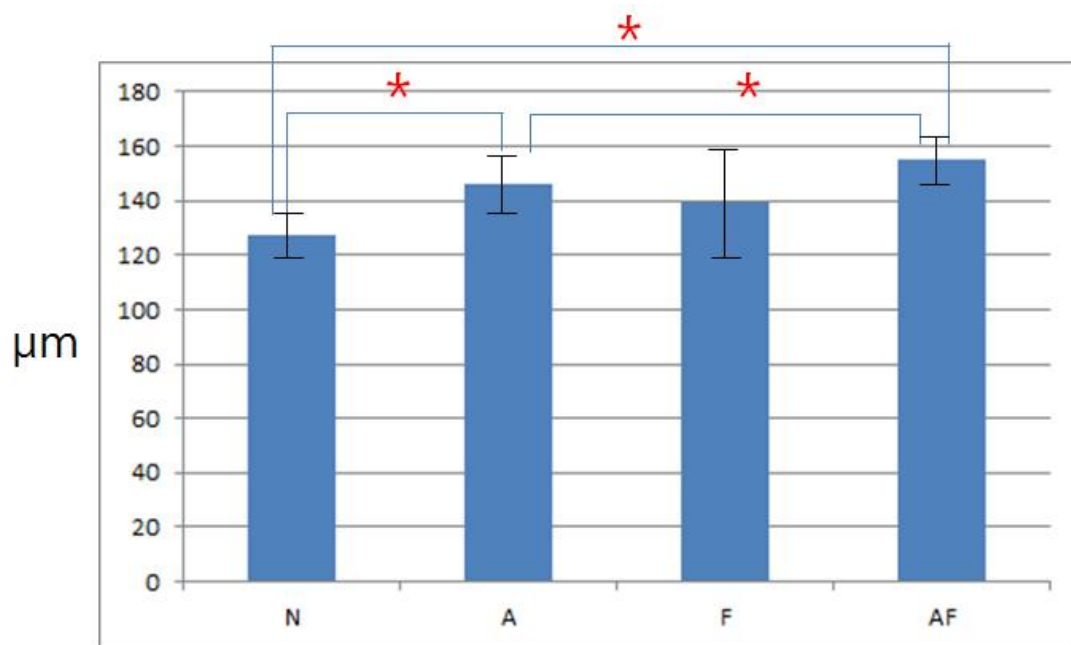


Figure 6. Dermal thickness. The dermal thickness, as determined by hematoxylin & eosin staining, was significantly greater in both the ADSC group and ADSC with fat than in the other groups ( $p = 0.04$  and  $p = 0.03$ , respectively). However, thickness did not differ significantly between the control group and the fat group ( $p = 0.19$ ).



# Collagen density

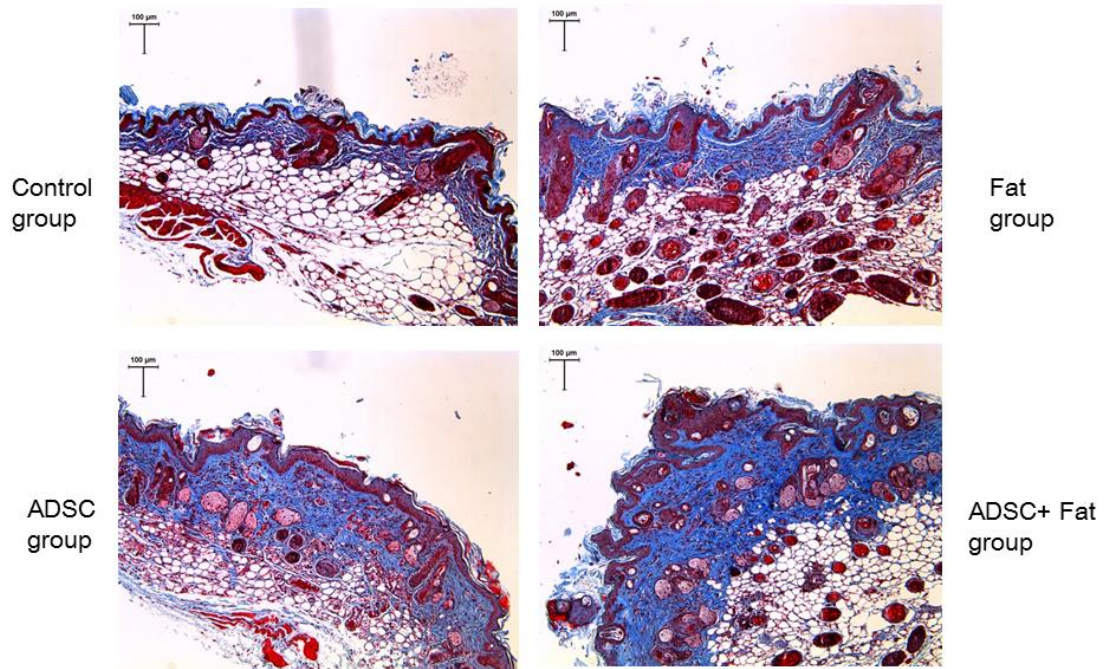


Figure 7. The density of collagen. The density of collagen exhibited similar patterns in all groups to the dermal thickness patterns. The average densities of collagen according to an image-based analysis of Masson's trichrome staining were  $52.3 \pm 8.2\%$  in the ADSC group,  $39.5 \pm 8.6\%$  in the fat group, and  $60.0 \pm 12.4\%$  in the ADSC with fat group.

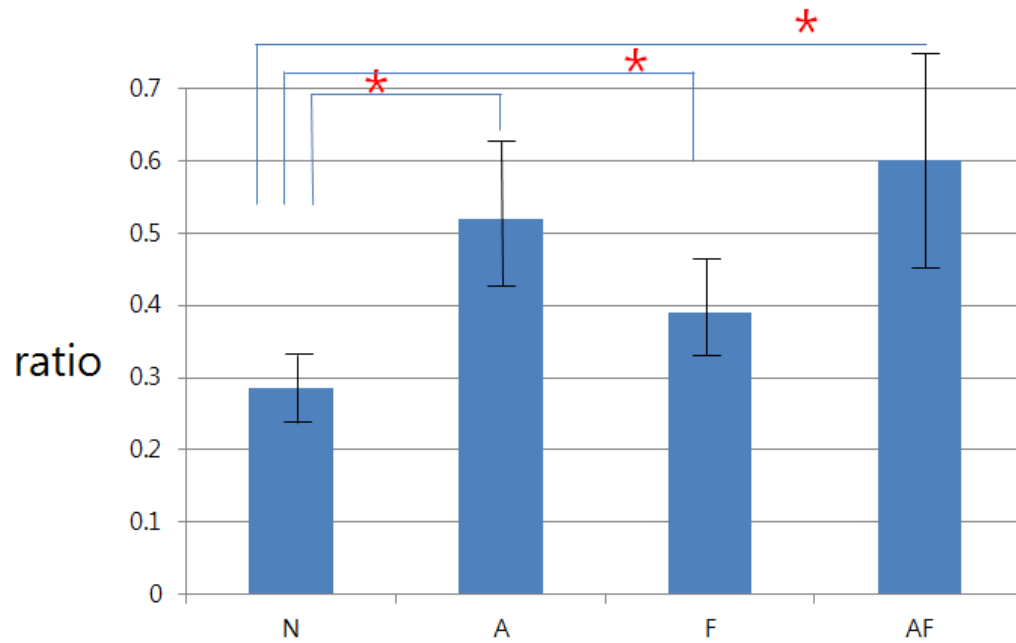


Figure 8. The density of collagen. The densities of collagen were significantly elevated in both ADSC group and ADSC with fat group (ADSC group,  $p < 0.01$ ; ADSC with fat group,  $p < 0.01$ ). However, collagen density did not differ significantly between the fat group and the ADSC with fat group ( $p = 0.21$ ).

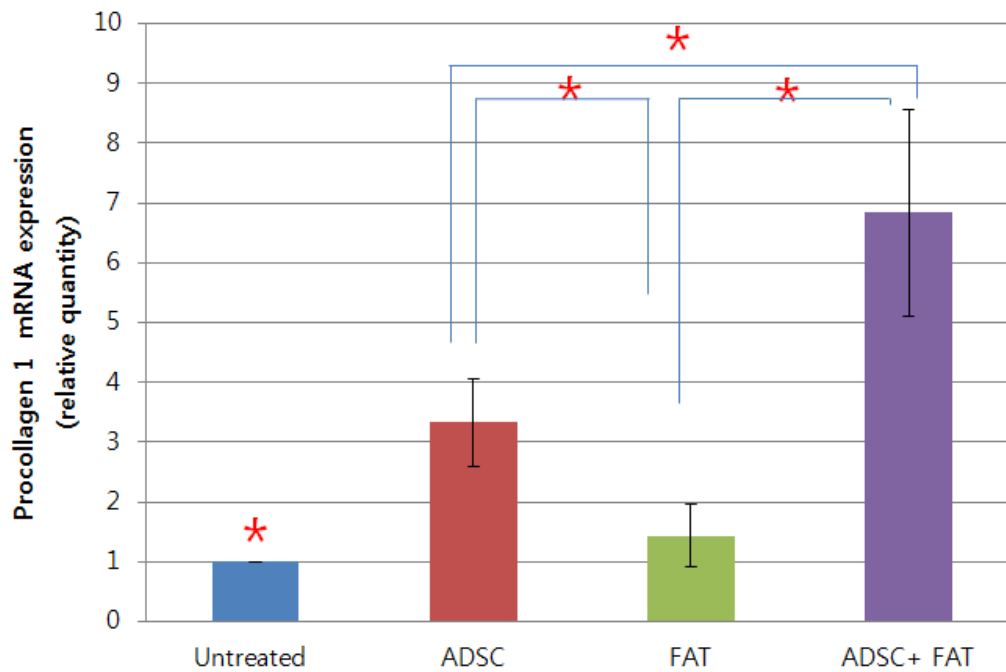


Figure 9. Type I procollagen mRNA. Real-time PCR revealed that the levels of type I procollagen increased in all 3 experimental groups compared with the control group. The ratio for the ADSC group relative to the control group was  $3.2 \pm 0.5$  ( $p < 0.01$ ) and for the fat group relative to the control group was  $1.4 \pm 0.3$  ( $p = 0.04$ ). Type I procollagen mRNA levels in the ADSC with fat group were statistically significantly higher than those in the ADSC group and fat group ( $p = 0.01$ ,  $p < 0.01$ , respectively).

# Tropoelastin

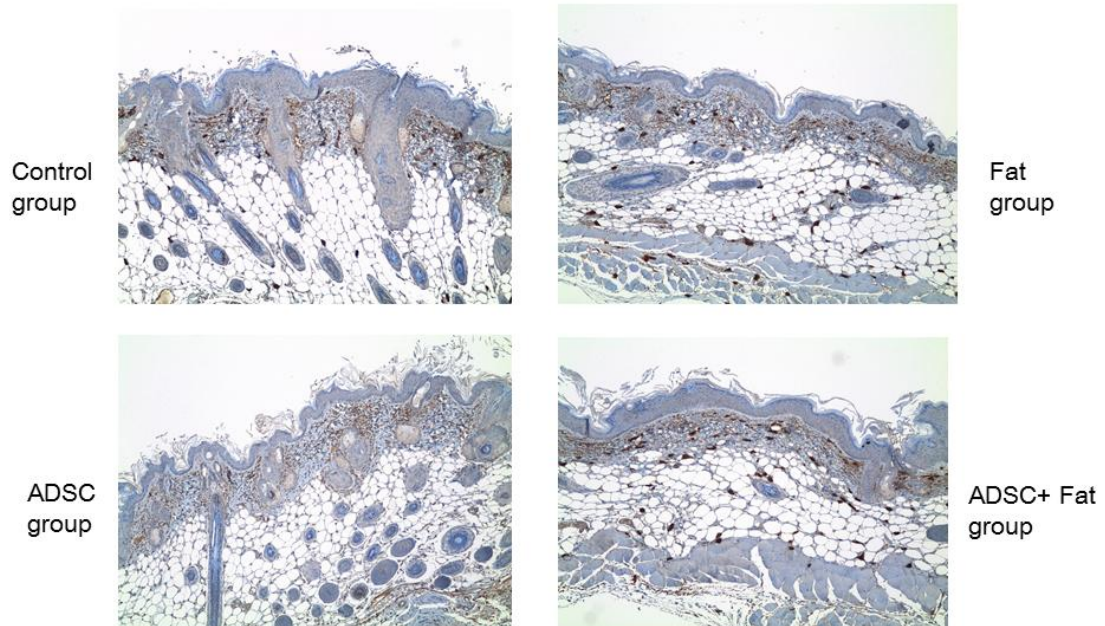


Figure 10. Tropoelastin. The amount of tropoelastin decreased after ADSC injection.

Moreover, the amount of tropoelastin was significantly lower after ADSC with fat injection. However, there was no statistically significant difference between the control group and the fat group.

# Fibrillin

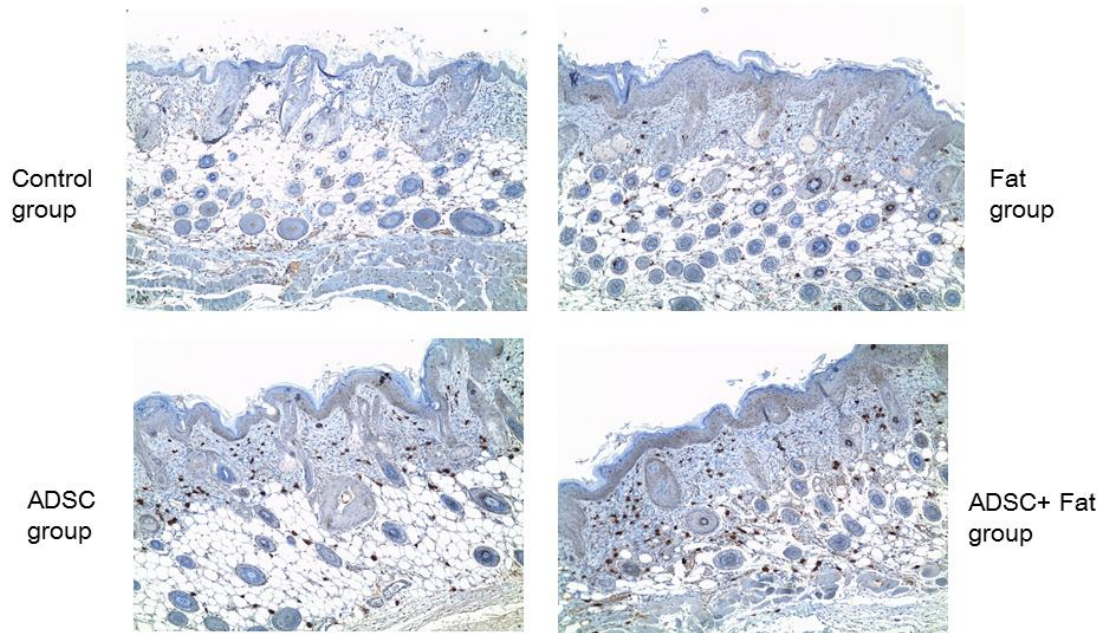


Figure 11. Fibrillin-1. Fibrillin-1 increased significantly after ADSC injection and ADSC with fat injection. However, there was no statistically significant difference between the control group and fat group.



# CD31

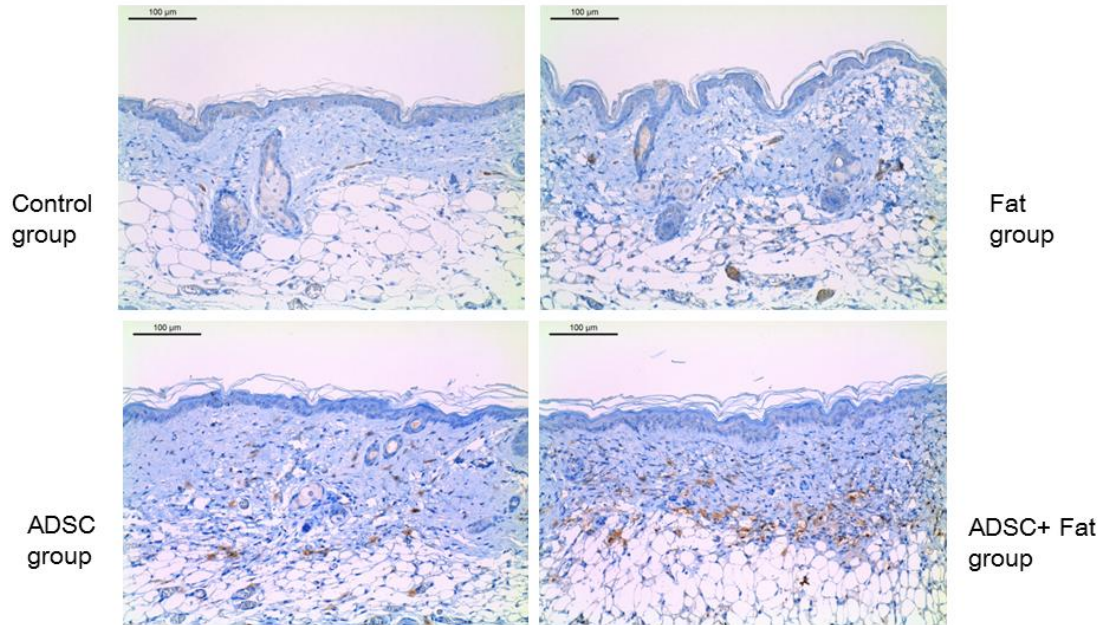


Figure 12. Expression of CD31. CD31 expression increased significantly in all three groups. CD31 expression in the ADSC with fat group differed significantly from those in the ADSC group and the fat group. The numbers of CD31-positive vessels in the ADSC with fat groups ( $31.8 \pm 6.4$ ) were significantly higher than those in the fat group ( $15.3 \pm 7.4$ ) ( $p = 0.02$ ).

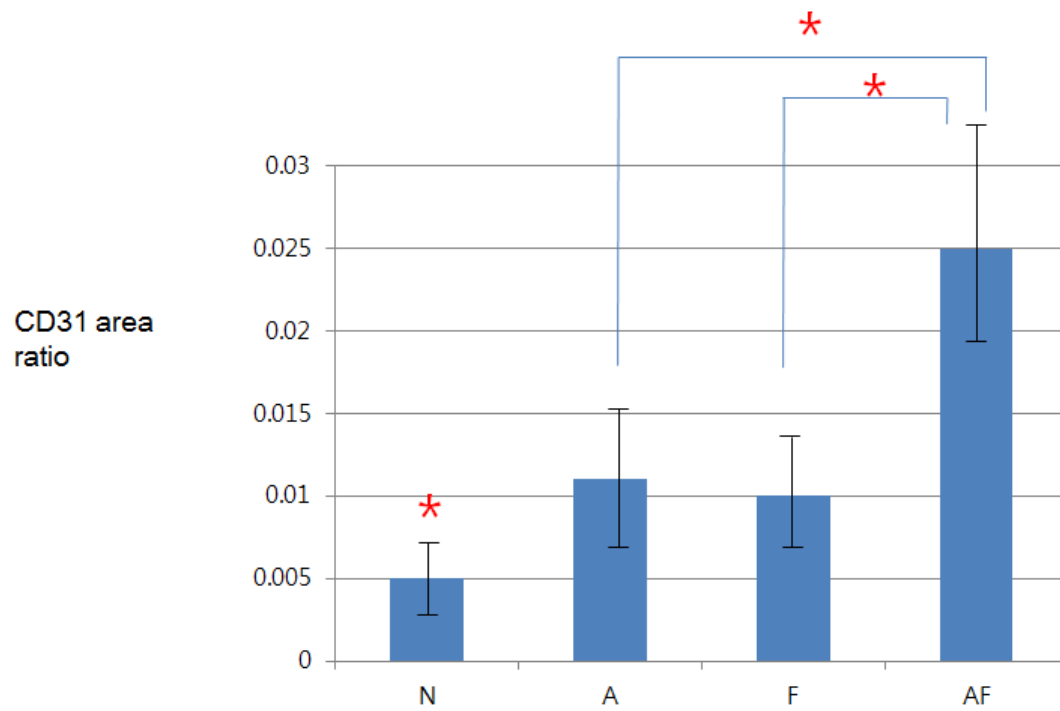


Figure 13. Expression of CD31. CD31 expression increased significantly in all three groups. CD31 expression in the ADSC with fat group differed significantly from those in the ADSC group and the fat group.

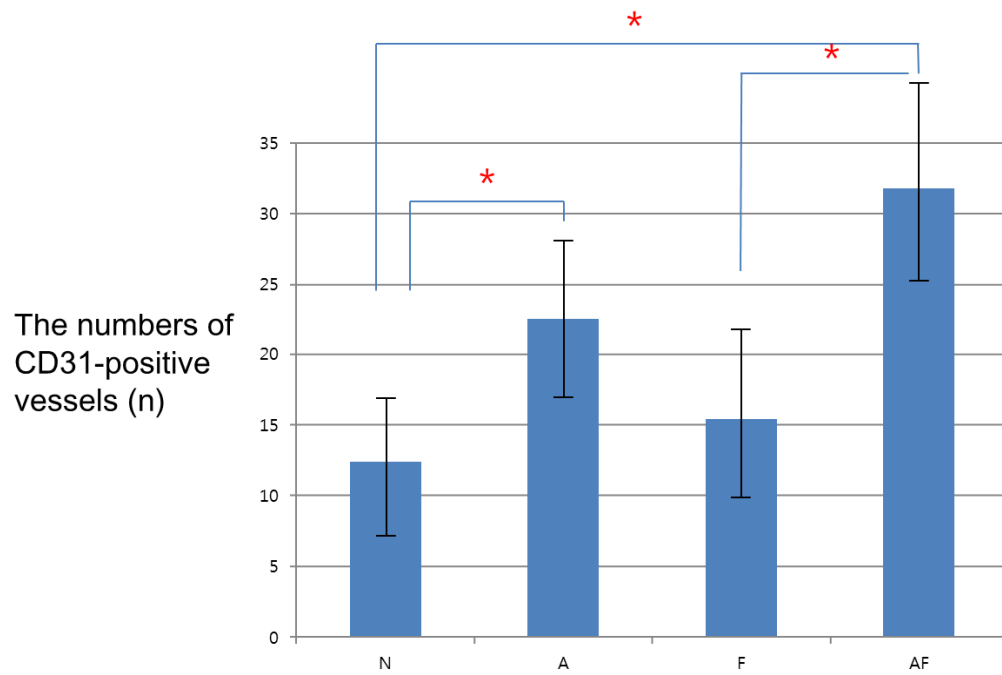


Figure 14. The numbers of CD31-positive vessels in the ADSC with fat group ( $31.8 \pm 6.4$ ) were significantly higher than those in the fat group ( $15.3 \pm 7.4$ ) ( $p = 0.02$ ).



## DISCUSSION

Fat graft has become one of the most common operations in the field of plastic surgery.<sup>28,29</sup> Basic research and clinical trials have evaluated methods beyond simple fat grafts.<sup>6-9,21</sup> Injections with ADSCs and fat have been actively studied. Since ADSCs could directly differentiate into adipocytes, increase collagen production, and activate fibroblasts, ADSCs have a wrinkle improvement effect.<sup>21</sup> The concept of a nanofat graft has recently been introduced and is the subject of recent research.<sup>30-34</sup> Nanofat is an emulsified suspension derived from fat tissue that is processed by mechanical means; it was reported by Tonnard et al.<sup>30</sup> Subsequent studies have demonstrated that nanofat contains a large quantity of ADSCs that retain an extensive proliferative and multipotent differentiation capacity.<sup>32</sup> Moreover, most nanofat studies have suggested that ADSCs play a major role in the outcomes, and interest in the effectiveness of ADSCs is increasing.<sup>33,34</sup> Hence, we verified the effect of the injection of fat tissue and ADSCs in comparison with the injection of fat tissue alone.

We proved that ADSCs activated collagen production and elastic fiber production. These findings are consistent with previous research.<sup>6-9,16,21,35</sup> ADSCs secrete a variety of cytokines that activate fibroblasts and increase collagen production.<sup>6-9,16,35</sup> However,

our results show that the direct injection of fat can have a similar effect as the injection of ADSCs, although the mechanism underlying these effects is unclear. The most distinctive finding was that ADSCs and fat have a synergic effect on collagen synthesis and neovascularization. The effects of ADSCs and fat were significantly different from those of fat alone and those of ADSC alone. Previous studies have shown that ADSC secretes growth factors such as VEGF, HGF, and TGF- $\beta$  and promotes angiogenesis through IL-6 expression.<sup>35-38</sup> In this experiment, we could hypothesize that ADSC stimulates collagen production by stimulating growth factors and interacts with fat to promote angiogenesis.

There was an increase in vessels, but this could be explained by either vessel engorgement or neovascularization. Therefore, we did not simply measure the vessel surface area, but also determined the number of vessels and changes in diameter.<sup>34</sup> In this study, the numbers of CD31-positive vessels in the ADSC with fat groups were significantly higher than those in the fat group, suggesting that our results could be explained by neovascularization. It is possible that the neovascularization resulted from proangiogenic growth factors, but further research is needed to confirm the mechanism underlying the synergic effects.

We believe that a major contribution of this study is the use of the chronologic aging model. Most studies of skin wrinkles have used a photo-aging model.<sup>2-5,39,40</sup> There are some key differences between the photo-aging and chronologic aging models. Photo-aging, unlike chronological aging, results in the active destruction of collagen and elastin fibers in the skin.<sup>2,39</sup> Some researchers therefore prefer the term “photo-damage” as a more accurate expression. There is debate regarding whether it accurately reflects the process of skin aging. Accordingly, to determine the effects of adipocytes and ADSCs on natural aging, the chronologic aging model was chosen. To establish the chronologic model, we performed replica tests at 4-week intervals and confirmed that the wrinkles stabilized after 48 weeks of age. We believe this is the first application of a chronologic model established using nude mice, and this study provides a basis for future studies of aging using human cells. The replica patterns in the photoaging model and chronologic model were different. A change in wrinkle depth was apparent in the photoaging model. The wrinkle area increased remarkably in the chronologic model. However, the chronological model required a long study duration of about 1 year, and a sufficient number of animals is needed to account for animal death during this period. This is a potential limitation of the model.

This study had several limitations. First, there are differences between the immune systems of mice and humans. Mice are considered good animal models for studying the chronological aging and photoaging of skin.<sup>3-5,39</sup> Established wrinkle models utilize hairless mice, and various analyses of filler and cell injections used these models.<sup>2-5,39,40</sup> However, for clinical applications, it may be appropriate to use nude mice for xenograft research involving human cells.<sup>21</sup> Second, the injected volumes varied from group to group. At the time of planning the experiment, we had set up 3 experimental groups with one control group instead of comparing two groups like A vs B. So there can be a reasonable doubt that there could be a volume effect with ADSC plus fat group, because this group has received more volume than other groups. However, in the case of ADSC, the cell did not occupy 0.5 cc, but the volume occupied by the cells was insignificant and diluted in 0.5 cc of Hank's Balanced Salt Solution (HBSS). Though this solution is absorbed in the body over a period of several hours to several days, we can't completely rule out the possibility that the injected volume would have some effects on this experiment to determine the results especially in skin replica analysis. Third, we investigated simple cell injections, but the injection of growth factors and other injection types may have different effects. Forth, we evaluated the time from injection to the most pronounced effects in order to determine the ideal interval between repeat fat

injections in the clinical setting; however, parameters were only measured at the predetermined endpoints.

## **CONCLUSION**

ADSCs and fat both have the potential to play an important role in wrinkle reduction and have a synergic effect on collagen synthesis and neovascularization.

## REFERENCES

1. Fallacara A, Manfredini S, Durini E, Vertuani S. Hyaluronic acid fillers in soft tissue regeneration. *Facial Plast Surg.* 2017;33(1):87–96.
2. Fisher GJ, Kang S, Varani J, Bata-Csorgo Z, Wan Y, Datta S, et al. Mechanisms of photoaging and chronological skin aging. *Arch Dermatol.* 2002;138(11):1462-1470.
3. Bhattacharyya TK, Thomas JR. Histomorphologic changes in aging skin. Observations in the CBA mouse model. *Arch Facial Plast Surg.* 2004;6(1):21-25.
4. Kim HH, Lee MJ, Lee SR, Kim KH, Cho KH, Eun HC, et al. Augmentation of UV-induced skin wrinkling by infrared irradiation in hairless mice. *Mech Ageing Dev.* 2005;126(11):1170-1177.
5. Kligman LH. The hairless mouse model for photoaging. *Clin Dermatol.* 1996;14(2):183-195.
6. Kim WS, Park BS, Sung JH, Yang JM, Park SB, Kwak SJ, et al. Wound healing effect of adipose-derived stem cells: a critical role of secretory factors on human dermal fibroblasts. *J Dermatol Sci.* 2007;48(1):15-24.

7. Kim WS, Park BS, Kim HK, Park JS, Kim KJ, Choi JS, et al. Evidence supporting antioxidant action of adipose-derived stem cells: protection of human dermal fibroblasts from oxidative stress. *J Dermatol Sci.* 2008;49(2):133-142.
8. Kim WS, Park BS, Park SH, Kim HK, Sung JH. Antiwrinkle effect of adipose-derived stem cell: activation of dermal fibroblast by secretory factors. *J Dermatol Sci.* 2009;53(2):96-102.
9. Kim WS, Park BS, Sung JH. Protective role of adipose-derived stem cells and their soluble factors in photoaging. *Arch Dermatol Res.* 2009;301:329-336.
10. Courderot-Masuyer Carol, Robin Sophie, Tauzin He'le'ne, Humbert Philippe. Evaluation of the behaviour of wrinkles fibroblasts and normal aged fibroblasts in the presence of poly- L-lactic acid. *J Cosm Dermatol Sci Appl.* 2012;2:20-27.
11. Smith SR, Munavalli G, Weiss R, Maslowski JM, Hennegan KP, Novak JM. A multicenter, double-blind, placebo-controlled trial of autologous fibroblast therapy for the treatment of nasolabial fold wrinkles. *Dermatol Surg.* 2012;38:1234-1243.
12. Munavalli GS, Smith S, Maslowski JM, Weiss R. Successful treatment of



- depressed, distensible acne scars using autologous fibroblasts: a multi-site, prospective, double blind, placebocontrolled clinical trial. *Dermatol Surg.* 2013;39(8):1226-1236.
13. Topcu A, Aydin OE, Unlu M, Barutcu A, Atabey A. Increasing the viability of fat grafts by vascular endothelial growth factor. *Arch Facial Plast Surg.* 2012;14(4):270-276.
  14. Craft RO, Rophael J, Morrison WA, Vashi AV, Mitchell GM, Penington AJ. Effect of local, long-term delivery of platelet-derived growth factor (PDGF) on injected fat graft survival in severe combined immunodeficient (SCID) mice. *J Plast Reconstr Aesthet Surg.* 2009;62(2):235-243.
  15. Tamura E, Tabata Y, Yamada C, Okada S, Iida M. Autologous fat augmentation of the vocal fold with basic fibroblast growth factor: computed tomographic assessment of fat tissue survival after augmentation. *Acta Otolaryngol.* 2015;135(11):1163-1167.
  16. Kim JH, Jung M, Kim HS, Kim YM, Choi EH. Adipose-derived stem cells as a new therapeutic modality for ageing skin. *Exp Dermatol.* 2011;20(5):383-387.
  17. Yoshimura K, Sato K, Aoi N, Kurita M, Inoue K, Suga H, et al. Cell-assisted lipotransfer for facial lipoatrophy: efficacy of clinical use of adipose-derived

- stem cells. *Dermatol Surg.* 2008;34(9):1178-1185.
18. Laloze J, Varin A, Bertheuil N, Grolleau JL, Vaysse C, Chaput B. Cell-assisted lipotransfer: current concepts. *Ann Chir Plast Esthet.* 2017;62(2):609-616.
  19. Piccinno MS, Veronesi E, Loschi P, Pignatti M, Murgia A, Grisendi G, et al. Adipose stromal/stem cells assist fat transplantation reducing necrosis and increasing graft performance. *Apoptosis.* 2013;18(10):1274-1289.
  20. Yan XM, Seo MS, Hwang EJ, Cho IH, Hahn SK, Sohn UD. Improved synthesis of hyaluronic acid hydrogel and its effect on tissue augmentation. *J Biomater Appl.* 2012;27(2):179-186.
  21. Jeong JH, Fan Y, You GY, Choi TH, Kim S. Improvement of photoaged skin wrinkles with cultured human fibroblasts and adipose-derived stem cells: a comparative study. *J Plast Reconstr Aesthet Surg.* 2015;68(3):372-381.
  22. Lin T, Chao C, Saito S, Mazur SJ, Murphy ME, Appella E, et al. p53 induced differentiation of mouse embryonic stem cells by suppressing Nanog expression. *Nat Cell Biol.* 2005;7(2):165-171.
  23. Westermarck J, Holmström T, Ahonen M, Eriksson JE, Kahari VM. Enhancement of fibroblast collagenase-1 (MMP-1) gene expression by tumor promoter okadaic acid is mediated by stress-activated protein kinases Jun N-

terminal kinase and p38. *Matrix Biol.* 1998;17(8-9):547-557.

24. Howard EW, Crider BJ, Updike DL, Bullen EC, Parks EE, Haaksma CJ, et al. MMP-2 expression by fibroblasts is suppressed by the myofibroblast phenotype. *Exp Cell Res.* 2012;318(13):1542-1553.
25. Hattori N, Mochizuki S, Kishi K, Nakajima T, Takaishi H, D'Armiento K, et al. MMP-13 plays a role in keratinocyte migration, angiogenesis, and contraction in mouse skin wound healing. *Am J Pathol.* 2009;175(2):533-546.
26. Yun SJ, Yoon HY, Bae SC, Lee OJ, Choi YH, Moon SK, et al. Transcriptional repression of RUNX2 is associated with aggressive clinicopathological outcomes, whereas nuclear location of the protein is related to metastasis in prostate cancer. *Prostate Cancer Prostatic Dis.* 2012;15(4):369-373.
27. Kim SJ, Kim DC, Kim MC, Jung GJ, Kim KH, Jang JS, et al. Fascin expression is related to poor survival in gastric cancer. *Pathol Int.* 2012;62(12):777-784.
28. Bucky LP, Kanchwala SK. The role of autologous fat and alternative fillers in the aging face. *Plast Reconstr Surg.* 2007;120(6 Suppl):89S-97S.
29. Coleman SR. Long-term survival of fat transplants: controlled demonstrations. *Aesthetic Plast Surg.* 1995;19(5):421-425.
30. Tonnard P, Verpaele A, Peeters G, Hamdi M, Cornelissen M, Declercq H.

- Nanofat grafting: basic research and clinical applications. *Plast Reconstr Surg.* 2013;132(4):1017-1026.
31. Kemaloğlu CA. Nanofat grafting under a split-thickness skin graft for problematic wound management. *Springerplus.* 2016;5:138.
32. Banyard DA, Sarantopoulos CN, Borovikova AA, Qiu X, Wirth GA, Paydar KZ, et al. Phenotypic analysis of stromal vascular fraction after mechanical shear reveals stress-induced progenitor populations. *Plast Reconstr Surg.* 2016;138(2):237e-247e.
33. Yu Q, Cai Y, Huang H, Wang Z, Xu P, Wang X, et al. Co-transplantation of nanofat enhances neovascularization and fat graft survival in nude mice. *Aesthet Surg J.* 2017 Nov 17. doi: 10.1093/asj/sjx211
34. Xu P, Yu Q, Huang H, Zhang WJ, Li W. Nanofat increases dermis thickness and neovascularization in photoaged nude mouse skin. *Aesthetic Plast Surg.* 2018;42(2):343-351.
35. Charles-de-Sá L, Gontijo-de-Amorim NF, Maeda Takiya C, Borojevic R, Benati D, Bernardi P, et al. Antiaging treatment of the facial skin by fat graft and adipose-derived stem cells. *Plast Reconstr Surg.* 2015 Apr;135(4):999-1009.

36. Rehman J, Traktuev D, Li J, et al. Secretion of angiogenic and antiapoptotic factors by human adipose stromal cells. *Circulation*. 2004;109(10):1292-1298.
37. Dong Z, Peng Z, Chang Q, Lu F. The survival condition and immunoregulatory function of adipose stromal vascular fraction (SVF) in the early stage of nonvascularized adipose transplantation. *PLoS One*. 2013;8(11):e80364.
38. Pu CM, Liu CW, Liang CJ, Yen YH, Chen SH, Jiang-Shieh YF, et al. Adipose-Derived Stem Cells Protect Skin Flaps against Ischemia/Reperfusion Injury via IL-6 Expression. *J Invest Dermatol*. 2017 Jun;137(6):1353-1362.
39. Hwang KA, Yi BR, Choi KC. Molecular mechanisms and in vivo mouse models of skin aging associated with dermal matrix alterations. *Lab Anim Res*. 2011;27(1):1-8.
40. Varani J, Spearman D, Perone P, Fligiel SE, Datta SC, Wang ZQ, et al. Inhibition of type I procollagen synthesis by damaged collagen in photoaged skin and by collagenase-degraded collagen in vitro. *Am J Pathol*. 2001;158(3):931-942.

## 국문 초록

# 노화된 생쥐에서 지방줄기세포와 지방이식의 항피부노화 상승효과

**서론:** 지방이식만 시행했을 때와 지방이식과 지방줄기세포 주입을 동시에 시행했을 때의 주름 개선효과를 비교 분석하였다.

**방법:** 50주까지 자연노화 시킨 암컷 BALB / c 누드 마우스 44마리를 4 그룹으로 나누었다. 첫 번째 군은 음성 대조군이고, 한군에는 지방줄기세포 ( $1 \times 10^5$  cells, 0.5ml)를 다른 한군에는 지방(0.5ml)을 쥐 등에 주사했다. 마지막 군에는 지방(0.5ml)과 지방줄기세포 ( $1 \times 10^5$  cells, 0.5ml)를 복합 주입했다. 주입 4주후, 주름 복제본 분석(replica analysis)을 하고, 조직검사를 시행하여 진피 두께, 콜라겐 밀도를 측정하였다. 또한 중합효소연쇄반응과 웨스턴블롯검사를 통해 1형 콜라겐과 금속단백분해효소(matrix metalloproteinases) - 1, 2, 3, 9, 13을 측정 하고, 면역조직화학검사를 통해 쏫탄력소(tropoelastin)와 피브릴린(fibrillin)-1와 CD31을 평가하였다.

**결과:** 복제본 분석에서는 지방줄기세포 그룹과 복합주입 그룹 모두에서 주름이 감소하였다. 지방줄기세포 그룹에서는 콜라겐 생성이 촉진되었고, 특히 지방줄기세포와 지방을 같이 복합주입한 그룹에서 1형 procollagen 생성이 지방줄기세포 그룹과 지방 그룹 모두에 비해서 통계적으로 유의하게 증가하였다. CD31 발현도 3가지 실험군에서 모두 증가하였는데, 지방줄기세포와 지방을 같이 주입한 그룹에서 지방줄기세포 그룹과 지방 그룹 모두에 비해 모두 통계적으로 유의하게 증가하였다.

**결론:** 지방줄기세포와 지방이식은 주름 감소에 중요한 역할을 하며, 같이 주입했을 때 콜라겐 합성과 혈관 신생의 시너지 효과가 있음을 확인하였다.

---

**주요어 :** 줄기세포, 중배엽 줄기세포, 지방이식, 노화

**학 번 :** 2011-30537